OPEN ACCESS
JOURNAL OF ADVANCED DIELECTRICS
Vol. 12, No. 1 (2022) 2160023 (8 pages)
© The Author(s)
DOI: 10.1142/S2010135X21600237

Structure, microstructure, dielectric and piezoelectric properties of $(1-x-y)BiFeO_3$–$xPbFe_{0.5}Nb_{0.5}O_3$–$yPbTiO_3$ ceramics

E. I. Sitalo*,§, N. A. Boldyrev*, L. A. Shilkina*, A. V. Nazarenko†, A. V. Nagaenko‡ and L. A. Reznichenko*

*Research Institute of Physics, Southern Federal University
No 194 Stachki Ave., Rostov-on-Don 344090, Russia

†Southern Scientific Center of RAS
No. 41 Chekhov Ave., Rostov-on-Don 344006, Russia

‡Institute of High Technology and Piezo Technic, Southern Federal University,
No 10 Milchakov St., Rostov-on-Don 344090, Russia

§sitalo@sfedu.ru

Received 18 April 2021; Revised 23 June 2021; Accepted 6 July 2021; Published 6 November 2021

Ceramics of quasi-binary concentration section ($x = 0.50$, $0.1 \le y \le 0.2$, $\Delta y = 0.025$) of the ternary solid solution system $(1-x-y)BiFeO_3$–$xPbFe_{0.5}Nb_{0.5}O_3$–$yPbTiO_3$ were prepared by the conventional solid-phase reaction method. By using X-ray diffraction technique, the phase diagram of the system was constructed, which was shown to contain the regions of cubic and tetragonal symmetry and the morphotropic phase boundary between them. Grain morphology, dielectric and piezoelectric properties of the selected solid solutions were investigated. The highest piezoelectric coefficient $d_{33} = 260$ pC/N was obtained. Dielectric characteristics of ceramics revealed ferroelectric relaxor behavior, a region of diffuse phase transition from the paraelectric to ferroelectric phase in the temperature range of 350–500 K.

Keywords: Dielectric properties; perovskites; multiferroics; piezoelectric properties; solid solutions.

1. Introduction

Multiferroics with coexisting electric, magnetic or elastic ordering are currently among the most intensively studied objects in materials science[1] due to the wide range of their possible applications, including the production of alternating and permanent magnetic field sensors, memory elements and spintronic devices.[2–4] Lead iron niobate $PbFe_{0.5}Nb_{0.5}O_3$ (PFN) is a well-known multiferroic with a perovskite-type structure having general chemical formula $A(B'_{0.5}B''_{0.5})O_3$ and the diffuse phase transition from the paraelectric (PE) to the ferroelectric (FE) phase at $T_C \sim 370$ K. FE and antiferromagnetic (AFM) ordering coexist in it only below $T_N \sim 120$–150 K, where T_N is a Neel temperature.[5] Bismuth ferrite $BiFeO_3$ (BF) is also multiferroic with $T_C \sim 1103$ K, $T_N \sim 643$ K and the G-type antiferromagnetism with incommensurate cycloidal magnetic ordering in the [110] direction.[6] Both materials are currently considered as the basis for many magnetoelectric structures. However, their widespread using is limited by several factors. For bismuth ferrite, this is the difficulty of obtaining BF in a single-phase state and the extremely high electric coercive field (E_C) required for the reorientation of ferroelectric domains. In addition, both PFN and BF are characterized by increased electrical conductivity caused by the presence of ions of variable valence (Fe^{2+}/Fe^{3+}) and oxygen vacancies in their structure. Nevertheless, modification[7,8] or creation of solid solutions[9,10] based on BF or PFN make it possible to stabilize the structure and improve the characteristics of the obtained ceramics. For a long time, binary systems based on multiferroics have been the subject of active study, and a lot of attention is paid to the $(1-x)BiFeO_3$–$xPbTiO_3$ system. The introduction of lead titanate $PbTiO_3$ (PT) stabilizes the perovskite phase and forms a morphotropic phase boundary (MPB) near $x \sim 0.3$. In this area, the $(1-x)$BF–xPT system demonstrates rather high piezoelectric characteristics, but at the same time retains a high electrical conductivity. In this regard, in recent years, considerable attention has been paid to obtaining new multiferroic materials by creating solid solutions of ternary systems based on BF and PT.[11–16] One of the most promising systems is the $(1-x-y)$BF–xPFN–yPT ternary system, in which, according to the literature data[16,17] and our preliminary studies,[18] there is MPB with coexisting rhombohedral (Rh) and tetragonal (T) phases. As is known, materials with MPB can demonstrate extreme properties and improve the electrophysical characteristics of the studied

§Corresponding author.

This is an Open Access article published by World Scientific Publishing Company. It is distributed under the terms of the Creative Commons Attribution 4.0 (CC BY) License which permits use, distribution and reproduction in any medium, provided the original work is properly cited.

ceramic. It was previously found[16] that, in the region of the phase diagram with a high PFN concentration (composition 0.25BF–0.63PFN–0.12PT), the samples of this system exhibit relatively high piezoelectric activity (up to 350 pC/N) and demonstrate high values of residual polarization at relatively low coercive field. In this regard, it is important to establish the regularities of the formation of structural, microstructural, dielectric, and piezoelectric characteristics of samples of the ternary system (1−*x*−*y*)BF–*x*PFN–*y*PT in the region of the phase diagram with a high PFN content.

2. Experimental Methods

Ceramic samples of the ternary system (1−*x*−*y*)BF–*x*PFN–*y*PT ($x = 0.50$, $0.1 \le y \le 0.2$, $\Delta y = 0.025$) were fabricated using conventional ceramic technology by double solid-phase synthesis at temperatures $T_1 = 1093$ K and $T_2 = 1143$ K depending on composition and holding times $\tau_1 = \tau_2 = 10$ h with following sintering at $T_{sin} = 1273$ K for 2 h. Bi_2O_3, Fe_2O_3, PbO, TiO_2, Nb_2O_5 with the content of the main substance not less than 99.95% were the initial reagents. Samples for sintering were pressed in the form of disks with the diameter of 10 mm and a thickness of 1 mm. After polishing, the electrodes were deposited onto the flat surfaces of the disks by stepwise firing of the silver paste at 473 K for 20 min, 773 K for 30 min and 1073 K for 20 min.

X-ray studies were carried out using a diffractometer DRON-3 (Bragg-Brentano focusing, filtered $Co_{K\alpha}$-radiation). The diffraction peak profile was approximated by the Lorentz function. The error in measuring the parameters *a*, *b*, *c* and volume, *V*, of the unit cell is $\Delta a = \Delta b = \Delta c = \pm(0.002–0.004)$ Å, $\Delta V = \pm 0.1$ Å^3. The modulation wavelength, Λ, was calculated by the formula:

$$\Lambda = \left| \left(\frac{1}{d_{hkl}} - \frac{1}{d_c} \right) \right|^{-1}, \quad (1)$$

where d_{hkl} and d_c are the interplanar distances of the main peak and satellite, respectively.[19]

The evaluation of the mechanical properties of the studied ceramics was carried out by a static method associated with a constantly increasing effect on the sample of an external uniaxial load. The value of the mechanical strength in static compression (s_{com}) was determined on a UTS-101-501-U (TestSystems, Russia). The test sample was squeezed through the grinded metal spacers of the device. The study of the ceramic grain structure was carried out using the KEYENCE VK-9700 color laser scanning 3D microscope.

Temperature dependences of the complex dielectric permittivity $\varepsilon^* = \varepsilon' - i\varepsilon''$ (ε' and ε'' are the real and imaginary parts of ε^*, respectively) were measured at $T = (300–900)$ K in the frequency range (10 Hz–100 kHz) using a computer-controlled broadband dielectric spectrometer Novocontrol Concept 40 during continuous cooling or heating of the sample at a rate of 2–3 K/min. Samples were polarized at $T = 400$ K in the polyethylene siloxane fluid under applied fields of 3–6 kV. Piezoelectric coefficients of the samples were measured at $f = 110$ Hz using quasistatic YE2730A d_{33} METER (APC International Ltd, USA).

3. Results and Discussion

X-ray phase analysis at room temperature showed that all studied solid solutions crystallize in the perovskite structure without foreign phases (Fig. 1(a)). The initial solid solution with $y = 0$ (binary system 0.5BF–0.5PFN) contains traces of the pyrochlore phase, which disappears after the introduction of PT. Figure 1(b) shows the diffraction peaks (111), (200), (211) and (220) on an enlarged scale along the 2θ axis. Two features of the X-ray diffraction patterns of solid solutions can be noted. The first is the concentration of diffuse scattering near the main diffraction peaks. This feature is a sign of

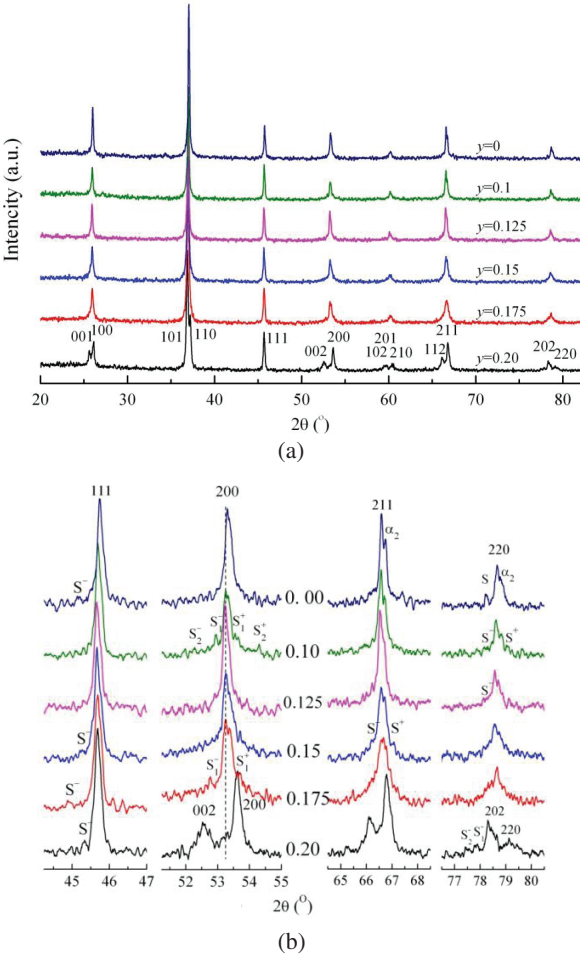

Fig. 1. (a) X-ray diffraction patterns of the solid solutions (1−*x*−*y*)-BF–*x*PFN–*y*PT. (b) Diffraction peaks (111), (200), (211) and (220) on an enlarged scale along the 2θ axis, S^-, S^+ are satellites of diffraction peaks from the side of smaller and larger angles 2θ, respectively.

segregation of atoms of the same type. And the second is the bifurcation of the (200) peak in solid solutions with $y = 0.10$, 0.15, 0.175, which may indicate the existence of two coherently coupled phases with the same symmetry and very close unit cell parameters. Solid solution 0.5BF–0.5PFN has cubic symmetry with unit cell parameter $a = 3.992$ Å. In the X-ray diffraction pattern of this solid solution, near the diffraction peak 220 from the side of smaller angle 2θ, a peak denoted by S is visible (Fig. 1(b)). Considering that the other diffraction peaks of this solid solution are single, the appearance of the S peak is not associated with a decrease in the symmetry of the crystal lattice. We suppose that is a consequence of the modulation of the structure by a wave of the density of defects in the <110> direction.

In the perovskite structure, which contains ions with variable valence (Nb and Ti) in the B position, there are planar defects such as planes of the crystallographic shift. When they are ordered, the structure is modulated in the direction perpendicular to the plane of the crystallographic shift.[20] As a result, satellites appear on the X-ray diffraction pattern near the diffraction peaks. Figure 1(b) also shows that the profiles of the diffraction peaks of solid solutions with $y = 0.10$, 0.15, 0.175 are strongly distorted by diffuse scattering. In this case, the peaks themselves are not split, except for the (200) peak, as noted above. In a solid solution with $y = 0.20$, the diffraction peaks split in accordance with the tetragonal distortion of the unit cell, and the diffuse maximum between peaks 002 and 200 may indicate the presence of a certain amount of a cubic phase in the sample. Thus, the phase diagram of the (1–x–y)BF–xPFN–yPT system in the studied region has the following form: the cubic phase remains in the range $0.0 \le y \le 0.20$, the tetragonal phase exists in the range $0.15 < y \le 0.20$, at $0.15 < y \le 0.20$ these phases coexist.

At some concentrations (Fig. 1(b)) of PT, the diffuse scattering transforms into satellite maxima. For example, at $y = 0.1$, near the peak (200), one can see symmetric satellites S^- and S^+. The modulation wavelengths, calculated from the position of clearly visible satellites S_1^- and S_2^+, are $\Lambda_1 = 340$ Å, $\Lambda_2 = 113$ Å, $\Lambda_2 = 1/3\Lambda_1$, which indicates domain-like modulation of the crystal lattice. The wavelengths of modulation in the directions <100>, <110> and <111>, calculated from the position marked in Fig. 1(b) satellites of diffraction peaks, respectively, (200), (220), (111) are shown in Table 1.

The data from the table shows that the crystal lattice of solid solutions is characterized by multiwave modulation. Thus, in a solid solution with $y = 0.10$, the modulation is realized in the <100> direction, which is characteristic of titanates of alkaline earth metals and lead with a perovskite structure.[21] In the <110> direction, two modulation waves are realized, the lengths of which are not related to each other, which is typical for the block structure of the oxygen framework of sodium and potassium niobates.[20] Based on this, it can be concluded that solid solutions are not homogeneous but consist of regions that differ in their real (defect) structure and chemical composition.

Table 1. Direction and length of the modulation wave in the studied ceramics.

	<100>		<110>		<111>
Y	Λ (S^-), Å	Λ (S^+), Å	Λ (S^-), Å	Λ (S^+), Å	Λ (S^-), Å
0.000			306		198
0.100	340	113	315	293	
0.125			294		
0.150					288
0.175					144
0.200			297; 168		327

Figure 2 shows the dependences of the parameters, unit cell volume and half-width of a single diffraction peak (111) of the samples on the PT concentration. The parameters and volume of the unit cell do not change with increasing y, as expected, since the ionic radii of the interchangeable ions are very close. A small increase in V at $y = 0.125$ does not exceed the measurement error and may be due to the lower defectiveness of the structure of this solid solution compared to other solid solutions of the ternary system. A significant increase in the half-width of the diffraction peak (111) at $y = 0.15$ and $y = 0.175$ is unambiguously associated with the appearance of clusters of the tetragonal phase.

It can be concluded that as the PT concentration increases, titanium ions are not statistically distributed in the matrix lattice (BF–PFN), but form segregations (clusters) with tetragonal symmetry of the crystal lattice. With increasing y, the size of the clusters increases, and at $y = 0.20$, a transition to the tetragonal phase occurs with a small, at the level of measurement error, jump in the unit cell volume $\Delta V = -0.05$ Å^3. Analysis of X-ray diffraction patterns of the studied solid solutions showed that the regions with different chemical

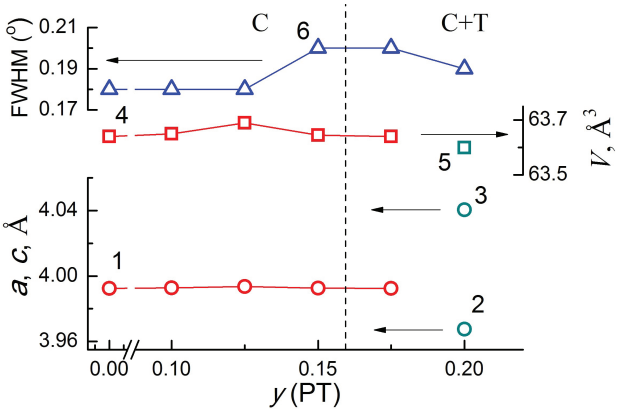

Fig. 2. Concentration dependences of parameters and volume of cubic and tetragonal unit cell: a (C) — (1), a (T) — (2), c (T) — (3), V (C) — (4), V (T) — (5) and FWHM — (6) of the (1–x–y)-BF–xPFN–yPT ceramics.

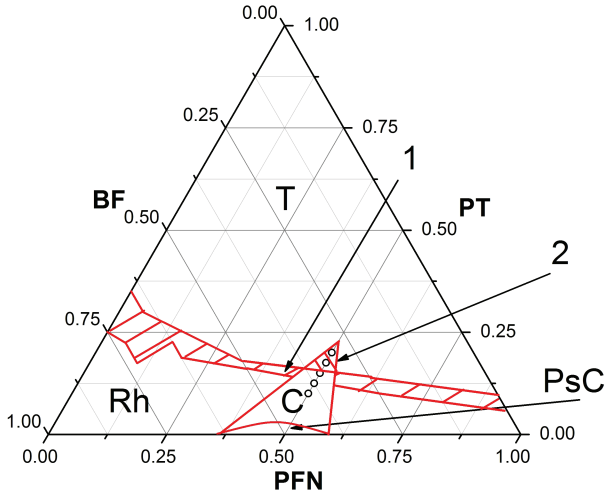

Fig. 3. Phase diagram of the ternary system (1–*x*–y)BF–*x*PFN–*y*PT: 1 — the first MPB (Rh+T), 2 — the second MPB (C+T).

compositions are most evenly distributed in the solid solution with $y = 0.125$. This is evidenced by the least distorted diffuse scattering profiles of the diffraction peaks and the absence of splitting of the diffraction peak (200).

Using the obtained data and Ref. 22, it is possible to refine the phase diagram of the system, obtained earlier in Ref. 18 (Fig. 3). As can be seen from the figure, the phase diagram contains two adjacent MPBs (Rh+T and C+T).

Figure 4 shows the micrographs of cleaved samples of the studied ternary system. The microstructure of ceramics with $y = 0.10$ is moderately inhomogeneous (Fig. 4(a)) and consists mainly of large crystallites in the form of convex irregular polyhedrons. The cleavage occurs both along the grain boundary and along the grains themselves, which indicates that the strengths of the grains and grain boundaries (or intergranular interlayers) are approximately equal. Crystallite size, $\bar{D}$, varies from ~15 μm to ~25 μm. It should be noted that the micrographs of the cleavage of the sample with $y = 0.10$ (and the rest of the samples too) contain darker brown areas. The presence of these inclusions is a consequence of the composition fluctuations of the studied ceramics. The clusters with tetragonal symmetry, which were mentioned in the discussion of the XRD data, are most likely localized in these regions and have a rather strong effect on the characteristics of the samples.

With an increase in the PT concentration, the average grain size sharply decreases to 10 μm (Fig. 4(b)), the number of brown areas increases. The cleavage passes through the intergranular spaces, which indicates a higher, in comparison with the boundaries and intercrystalline interlayers, grain strength. In addition, in the sample with $y = 0.125$ one can observe traces of fluxes and intercrystalline layers that indicate the change in the way of sintering — from solid-phase to sintering with the participation of the liquid phase (LP). Low-melting Bi-containing compounds of eutectic origin formed during the synthesis process can be the main components of this LP. Another possible source of the appearance of the LP is the relatively low-melting lead oxide with a melting point of 838 °C (in the composition $0.5PbO–0.5TiO_2$[23]). This is confirmed by the fact that with a further increase in the PT concentration, the number of fluids increases.

Further enrichment of the solid solution with lead titanate ($0.15 \le y \le 0.20$) leads to a decrease in the size of grains of all types, an increase in the amount of fluxes and some hardening

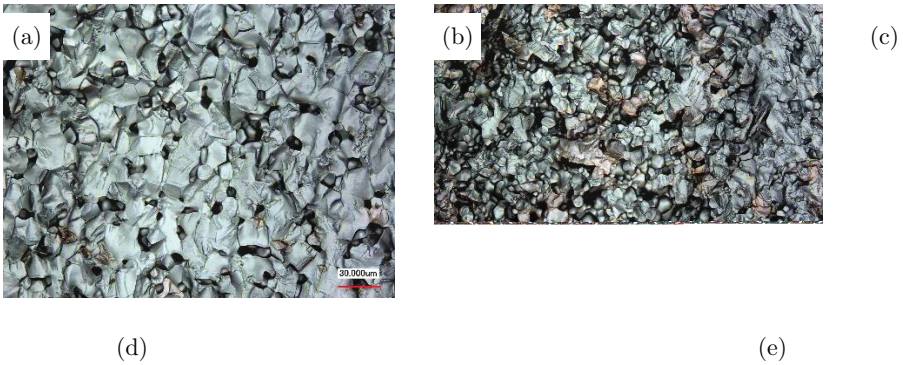

Fig. 4. Micrographs of chips of the studied ceramics: (a) $y = 0.10$, (b) $y = 0.125$, (c) $y = 0.15$, (d) $y = 0.175$, (e) $y = 0.20$.

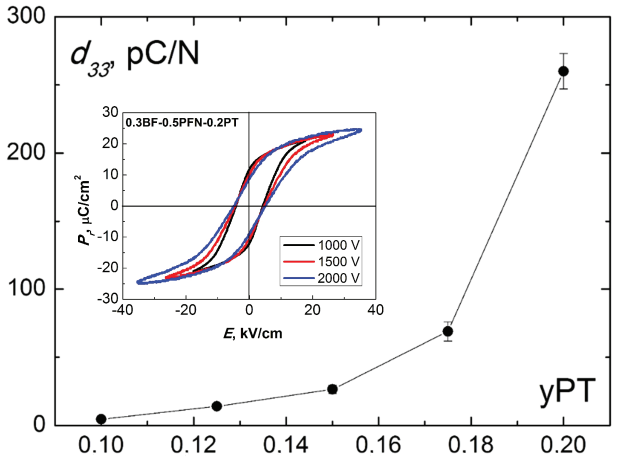

Fig. 7. Dependence of the piezomodule d_{33} on the PT concentration. Inset: Ferroelectric hysteresis loops of 0.3BF–0.5PFN–0.2PT ceramics.

4. Conclusion

Ceramic samples of solid solutions of the ternary system $(1-x-y)BiFeO_3$–$xPbFe_{0.5}Nb_{0.5}O_3$–$yPbTiO_3$ (x = 0.50, $0.1 \le y \le 0.2$, $\Delta y = 0.025$) were prepared by the conventional solid-phase reaction method. Using X-ray studies, it was found that at $0.10 \le y \le 0.15$ the objects have a cubic crystal structure containing segregations (clusters) with tetragonal symmetry of the crystal lattice, and at $y = 0.175$, 0.20 a morphotropic phase boundary with coexisting T and C phases formed. The place of their localization, as shown by the analysis of the microstructure, is the dark brown areas on the surface of the studied ceramics. The study of the dielectric characteristics revealed the relaxor-like behavior of the studied ceramics, as well as the presence of a stable piezoelectric response in several samples under study. A diffuse phase transition, which corresponds to the first maximum on the $\varepsilon'/\varepsilon_0(T)$ dependences, occurs in the range 385–435 K in the clusters of the T phase ($0.10 \le y \le 0.15$) and in the tetragonal part of the morphotropic region (y = 0.175, 0.20). The second maximum on the $\varepsilon'/\varepsilon_0(T)$ dependences is associated with the effects of Maxwell–Wagner polarization and relaxation of charge carriers at the grain boundaries. In the several samples, it was possible to observe high and stable piezoelectric responses. The maximum values of the piezomodulus were observed in the 0.3BF–0.5PFN–0.2PT ceramics (~260 pC/N) from the morphotropic region. The results show that $(1-x-y)$BF–xPFN–yPT system is a promising material for future investigation in consideration of its multiferroic properties.

Acknowledgments

The study was carried out with the financial support of the Ministry of Science and Higher Education of the Russian Federation (State task in the field of scientific activity, scientific project No. 0852-2020-0032) (BAZ0110/20-3-07IF). Work was performed using the equipment of the Center for Collective Use "Electromagnetic, Electromechanical and Thermal Properties of Solids", Research Institute of Physics, Southern Federal University and Center for Collective Use of the Southern Scientific Center of the Russian Academy of Science (Rostov-on-Don, Russia).

References

[1]A. P. Pyatakov and A. K. Zvezdin, Magnetoelectric and multiferroic media, *Phys.-Uspekhi* **55**(6), 557 (2012).
[2]J. Zhai, Z. Xing, S. Dong, J. Li and D. Viehland, Detection of pico-Tesla magnetic fields using magneto-electric sensors at room temperature, *Appl. Phys. Lett.* **88**, 062510 (2006).
[3]S. Tehrani, J. M. Slaughter, M. Deherrera, B. N. Engel, N. D. Rizzo, J. John Salter, M. Durlam, R. W. Dave, J. Janesky, B. Butcher, K. Smith and G. Grynkewich, Magnetoresistive random access memory using magnetic tunnel junctions, *Proc. IEEE* **91**(5), 703 (2003).
[4]W. A. Borders, H. Akima, S. Fukami, S. Moriya, S. Kurihara, Y. Horio, S. Sato and H. Ohno, Analogue spin-orbit torque device for artificial-neural-network-based associative memory operation, *Appl. Phys. Express* **10**(1), 013007 (2008).
[5]Yu. N. Venevtsev, V. V. Gagulin and V. N. Lyubimov, *Ferroelectromagnets* (Nauka, Moscow, 1982).
[6]A. M. Kadomtseva, Yu. F. Popov, A. P. Pyatakov, G. P. Vorob'ev, A. K. Zvezdin and D. Viehland, Phase transitions in multiferroic $BiFeO_3$ crystals, thin-layers, and ceramics: Enduring potential for a single phase, room-temperature magnetoelectric "holy grail", *Phase Trans.* **79**(12), 1019 (2006).
[7]S. V. Khasbulatov, A. A. Pavelko, L. A. Shilkina, L. A. Reznichenko, G. G. Gadjiev, A. G. Bakmaev, M.-R. M. Magomedov, Z. M. Omarov and V. A. Aleshin, Phase composition, microstructure, and thermophysical and dielectric properties of multiferroic $Bi_{1-x}Dy_xFeO_3$, *Thermophys. Aeromech.* **23**(3), 445 (2016).
[8]N. A. Boldyrev, A. V. Pavlenko, L. A. Reznichenko, I. A. Verbenko, G. M. Konstantinov and L. A. Shilkina, Effect of lithium carbonate on the ferroelectric properties of lead ferroniobate ceramics, *Inorg. Mater.* **52**(1), 76 (2016).
[9]N. A. Boldyrev, A. V. Pavlenko, L. A. Shilkina, L. A. Reznichenko and A. I. Miller, Structure and dielectric characteristics of $(1-x)BiFeO_3$–$xPbTiO_3$ solid solutions, *Bull. Russ. Acad. Sci.: Phys.* **80**(6), 733 (2016).
[10]J. Zhuang, L.-W. Su, H. Wu, A. A. Bokov, M. Liu, W. Ren and Z.-G. Ye, Coexisting ferroelectric and magnetic morphotropic phase boundaries in Dy-modified $BiFeO_3$-$PbTiO_3$ multiferroics, *Appl. Phys. Lett.* **107**(18), 182906 (2015).
[11]J. Zhuang, J. Zhao, L.-W. Su, H. Wu, A. A. Bokov, W. Ren and Z.-G. Ye, Structure and local polar domains of Dy-modified $BiFeO_3$-$PbTiO_3$ multiferroic solid solutions, *J. Mater. Chem. C* **3**(48), 12450 (2015).
[12]Q. Lin, C. He and X. Long, Structural, electric and magnetic properties of $BiFeO_3$–$Pb(Mg_{1/3}Nb_{2/3})O_3$–$PbTiO_3$ ternary ceramics, *J. Electroceram.* **36**, 8 (2016).
[13]A. Ahlawat, S. Satapathy, R. J. Choudhary, M. K. Singh and P. K. Gupta, Observation of magnetoelectric coupling in $BiFeO_3$–$(Pb(Mg_{1/3}Nb_{2/3})O_3$–$PbTiO_3)$ composites, *Mater. Lett.* **181**, 123 (2016).
[14]J. J. Abhilash, S. Goel, A. Hussain and B. Kumar, Ferro-/pyroelectric response of 0.57BF–0.31PMN–0.12PT ternary ceramic faraway from morphotropic phase boundaries, *Ceram. Int.* **43**(18), 16676 (2017).

[15]W. Hu, X. Tan and K. Rajan, Piezoelectric ceramics with compositions at the morpho-tropic phase boundary in the $BiFeO_3$–$PbZrO_3$–$PbTiO_3$ ternary system, *J. Am. Ceram. Soc.* **94**, 4358 (2011).

[16]D. Pang, C. He, S. Han, S. Pan, X. Long and H. Tailor, A new multiferroic ternary solid solution system of $BiFeO_3$–$Pb(Fe_{1/2}Nb_{1/2})O_3$–$PbTiO_3$, *J. Eur. Ceram. Soc.* **35**, 2033 (2015).

[17]D. Pang, C. He and X. Long, Ferroelectric and antiferromagnetic properties of a ternary multiferroic $BiFeO_3$–$Pb(Fe_{1/2}Nb_{1/2})O_3$–$PbTiO_3$ single crystal, *Ceram. Int.* **42**(16), 19433 (2016).

[18]N. A. Boldyrev, A. V. Pavlenko, L. A. Shilkina, A. V. Nazarenko, A. A. Bokov, L. A. Reznichenko, A. G. Rudskaya and E. I. Panchenko, Structure, microstructure, dielectric and piezoelectric properties of $(1–x–y)BiFeO_3$–$xPbFe_{0.5}Nb_{0.5}O_3$–$yPbTiO_3$ ceramics, *Ceram. Int.* **45**(12), 14768 (2019).

[19]A. Guinier, *X-ray Diffraction of Crystals* (M .: Publishing House of Physics and Mathematics. Literature, 1961).

[20]L. A. Reznichenko, L. A. Shilkina, E. S. Gagarina, Yu. I. Yuzyuk, O. N. Razumovskaya and A. V. Kozinkin, Crystallographic shear in niobium oxides of different compositions, *Crystallogr. Rep.* **49**(5), 820 (2004).

[21]L. A. Reznichenko, L. A. Shilkina, S. V. Titov, O. N. Razumovskaya, V. V. Titov and S. I. Shevtsov, Defect structure of alkaline-earth, cadmium, and lead titanates, *Inorg. Mater.* **41**(5), 492 (2005).

[22]L. A. Shilkina, A. V. Pavlenko, L. A. Reznitchenko and I. A. Verbenko, Phase diagram of the system of $(1–x)BiFeO_{3–x}PbFe_{0.5}Nb_{0.5}O_3$ solid solutions at room temperature, *Crystallogr. Rep.* **61**(2), 262 (2016).

[23]B. Jaffe, W. R. Cook Jr. and H. Jaffe, *Piezoelectric Ceramics* (Academic Press, London and New York, 1971).

[24]A. Ya. Dantsiger, L. A. Reznitchenko, S. I. Dudkina, O. N. Razumovskaya and S. I. Shilkina, Correlation between the microstructure of ferroelectric ceramics and their chemical and phase composition, the degree of perfection of the crystal structure and the preparation conditions, *Ferroelectrics* **214**(1), 255 (1998).

[25]S. V. Titov, L. A. Shilkina, L. A. Reznichenko, S. I. Dudkina, O. N. Razumovskaya, S. I. Shevtsova and E. M. Kuznetsova, Structure clusterization preceding concentration phase transitions, *Tech. Phys. Lett.* **26**(9), 810 (2000).